Int J Clin Exp Pathol (2009) 2, 553-560
www.ijcep.com/IJCEP904001

Original Article

Immunoreactivity of ICAM-1 in Human Tumors, Metastases and Normal Tissues

Sarah H. Hayes and Gail M. Seigel

Department of Ophthalmology, Ross Eye Institute, University at Buffalo, Buffalo, NY

Received 06 April 2009; Accepted in revision 18 May 2009; Available online 10 June 2009

Abstract: Intercellular adhesion molecule-1 (ICAM-1) is implicated to play a role in cancer metastasis, and may serve as a diagnostic tool for tumor prognosis and progression as well as a target for therapeutic intervention. The aim of this study was to carry out a comprehensive survey of ICAM-1 immunoreactivity in normal, malignant and metastatic tissues. We assessed immunoreactivity of ICAM-1 in a total of 300 tissue cores from multiple tissue arrays of normal, malignant, and metastatic tissues by immunohistochemistry. We scored tissue samples for ICAM-1 immunoreactivity on a 0-3 scale, assessed the number of samples exhibiting infiltrating immune cells, and documented ICAM-1 immunoreactivity in some specific cell types. ICAM-1 expression in normal tissues was highest in spleen and absent in the cerebrum, peripheral nerves, pancreas, ovary, breast, uterus, cervix, prostate, lung, larynx, bone marrow, striated muscle, heart, mesothelium, esophagus, small intestine, colon and liver. In primary malignancies, lymphoid tissues received the highest average ICAM-1 score while connective tissue/skin had the lowest average ICAM-1 score. Of the metastatic tissues, those originating from the urinary tract had the highest average ICAM-1 score while those originating from glandular tissues had the lowest average ICAM-1 score. Metastases localized in lymphoid tissues had a higher average ICAM-1 score than those localized in non-lymphoid tissues. Since ICAM-1 is associated with a variety of cancer types and appears to play a role in cancer metastasis, our findings should serve as a helpful resource for investigations of ICAM-1 as a biomarker, as well as a target for therapeutic interventions.
Key Words: ICAM-1, immunohistochemistry, metastasis, tumor, tissue array

Introduction

Intercellular adhesion molecule-1 (ICAM-1) is a transmembrane glycoprotein belonging to the immunoglobulin superfamily of adhesion molecules [1]. It is composed of five extracellular Immunoglobulin G-like domains and a short cytoplasmic tail that associates with cytoskeletal proteins [2]. ICAM-1 is continuously expressed at low levels on various cell types including fibroblasts, endothelial cells, and some leukocytes and is also cytokine inducible [1]. During inflammatory and immune responses, ICAM-1 expressed on endothelial cells associates with lymphocyte function-associated antigen-1 (LFA-1) and macrophage antigen-1 (Mac-1) presented on leukocytes facilitating the invasion of damaged tissue by immune cells [2].

Although ICAM-1 plays an important role in the immune response, it has also been implicated to play a role in elucidating tumor prognosis and progression in various types of cancer [1, 3, 4]. ICAM-1 is expressed on the surface of many cancer cell types [1, 5, 6, 7, 8] and is also present in a soluble form circulating in the plasma of cancer patients at elevated levels [3, 4]. It has also been proposed that ICAM-1 may be involved in the process of cancer metastases, facilitating the spread of metastatic cancer cells to secondary sites [7, 9, 10, 11].

Given its association with many cancer types, ICAM-1 may serve as an important diagnostic tool for assessing the progression and prognosis of tumors. Although ICAM-1 expression has been documented in specific cancer types, a comprehensive survey of its expression in a wide variety of cancer types has not been performed. The aim of this study was to examine normal, malignant and metastatic human tissues to determine the

expression patterns of ICAM-1 and its association with tumor progression. We performed immunohistochemical analysis on a broad range of both normal and malignant human tissue samples in order to compare and contrast ICAM-1 expression amongst various normal tissue and tumor types.

Materials and Methods

Immunohistochemistry

Tissue arrays [MC961t, MT801t, MC803t, FDA995t] (US Biomax, Rockville, MD) were initially baked for 1hr at 60°C before being deparaffinized in xylene and rehydrated in graded alcohols. Sections were then boiled in 1x citrate buffer antigen retrieval solution (pH 6.0) for 30min. After cooling for 20min, sections were circled with a Pap pen and rinsed with 1x phosphate buffer saline with Tween 20 (TPBS). Sections were incubated in 3% H_2O_2 for 5min at room temperature followed by a high volume wash with TPBS for 5min. Sections were then incubated in primary antibody (4.16µg/ml rabbit anti-ICAM-1, Cell Signaling, Danvers, MA) for 1hr. After a high volume wash with TPBS, sections were incubated in goat anti-rabbit biotinylated secondary antibody (1µg/ml, Vector Laboratories, Buringame, CA) for 45min followed by another high volume wash with TPBS. Sections were then incubated for 20min with horseradish peroxidase-conjugated avidin (Elite kit, Vector Laboratories) and were then washed in a large volume of TPBS for 10min. A diaminobenzidine (DAB) kit was then used to detect the antigens by incubating the sections with DAB for 5min. After being rinsed in distilled deionized water, sections were counterstained with hematoxylin, rinsed in distilled water, and dehydrated in graded alcohols and xylene before being coverslipped and mounted with Permount. Sections were analyzed by light microscopy using a Nikon Eclipse E600 microscope and images were collected with a SPOT RT camera (Diagnostic Instruments, Inc.).

Data Analysis

After ICAM-1 immunostaining, individual cores were evaluated and scored for intensity of ICAM-1 immunoreactivity on a 0-3 rating scale. For consistency, a single observer scored all samples, and a second observer confirmed scores by spot-checking. A score of zero was given to tissues with no ICAM-1 staining, a score of 1 delineated weak ICAM-1 staining, a score of 2 was used for moderate ICAM-1 staining, and a score of 3 was given to tissues with strong ICAM-1 staining. The proportion of samples with ICAM-1 positive immune cell infiltrate was calculated to distinguish infiltrate from the tumor proper. Staining of immunoreactive infiltrating immune cells was not considered in the overall score given to each tumor type. ICAM-1 staining of specific cell types in normal tissues was also assessed.

Tissue types were grouped for analysis and the scores averaged to construct tables. Tumor and tissue types were grouped according to the organ system from which they originated. Specimens grouped in the Digestive category included tumors/tissues of the lip, cheek, tongue, esophagus, stomach, duodenum, intestines, colon, rectum and liver. Specimens of the bladder and kidney were grouped together as Urinary tumors/tissues, and samples of the lung, larynx, pharynx, nose, and throat were grouped together under the Respiratory category. The Female Reproductive category included tumors/tissues of the cervix, uterus, breast, ovary, and endometrium and the Male Reproductive category included those of the prostate and testes. Tumors/tissues of the brain were accordingly grouped together in the Brain category, as were specimens of the spleen and lymph nodes under the Lymphoid category.

Glandular tumors/tissues included those of the pancreas and thyroid and those that fell under the Connective Tissue/Skin category included samples from fatty tissue, fibrous tissue, mesentery, epiploon, bone, cartilage, and skin. Overall, there were 91 primary malignancy samples, 74 metastatic samples, 75 normal samples as well as a combined total of 60 neuroblastoma, nephroblastoma, retinoblastoma, and leukemia samples analyzed (Supplementary Table 1). All samples analyzed were of tissue cores from different cases/patients

Results

We examined a variety of normal, malignant and metastatic tissues by ICAM-1 immunohistochemistry and examples are shown in **Figure 1**. Normal human tonsil, which is known to express ICAM-1, was used as a

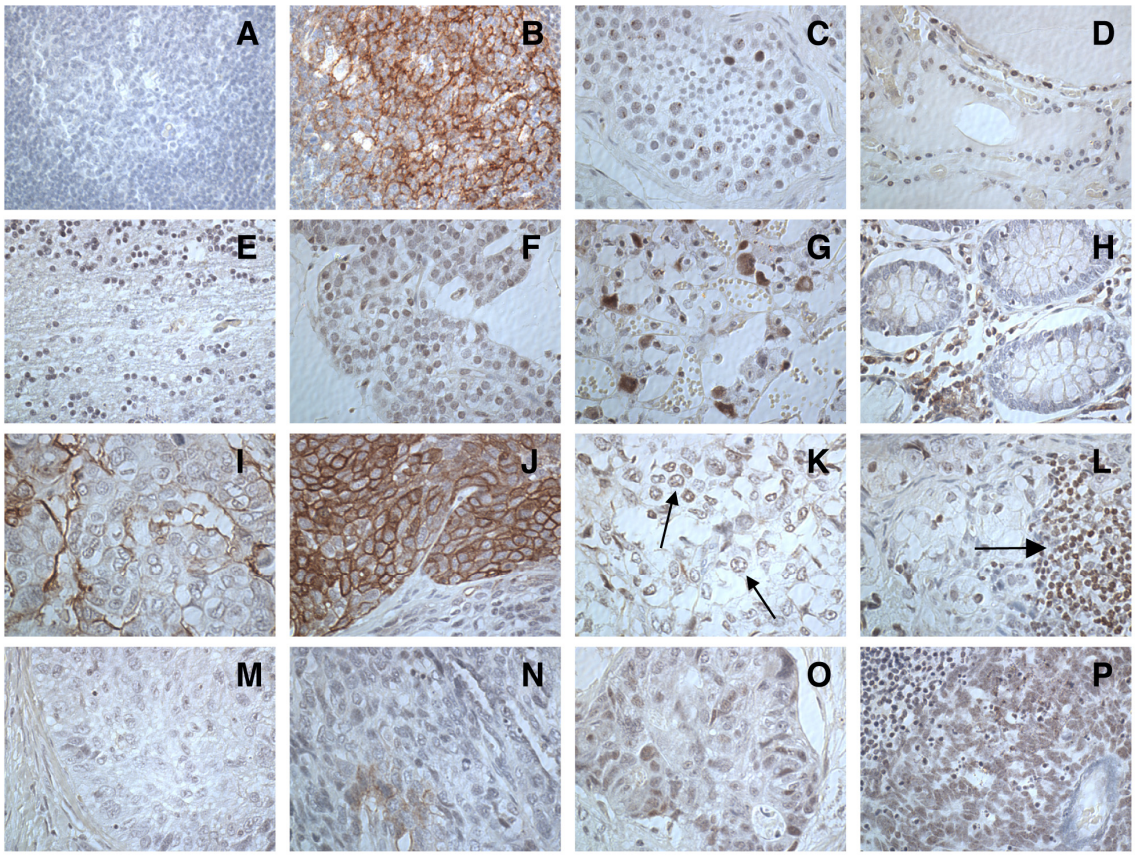

Figure 1 ICAM-1 immunoreactivity patterns in various normal tissue, tumor, and metastases samples. (**A**) Normal human tonsil treated with Rabbit IgG as negative control; (**B**) Normal human tonsil stained for ICAM-1 as positive control. Numbers in parentheses indicate ICAM-1 score of the tissue: (**C** - **H**) Normal human tissues expressing ICAM-1: **C**) Normal human testes (1+); **D**) Normal human thyroid (1+); **E**) Normal human cerebellum (2+); **F**) Normal human parathyroid (2+); **G**) Normal human pituitary (2+); **H**) Normal human colon (0). (**I** - **L**) Examples of various staining patterns seen in tumors and metastases: **I**) Adenocarcinoma of small intestine (3+); **J**) Metastatic squamous cell carcinoma from larynx found in lymph node (3+); **K**) Infiltrating ductal carcinoma of breast (2+). Arrows show perinuclear staining; **L**) Adenocarcinoma of prostate (2+). Arrow shows infiltrating cells positive for ICAM-1. (**M** - **P**) Examples of tumors with ICAM-1 scores 0-3: **M**) Metastatic squamous cell carcinoma in fibrous tissue from larynx found in the neck (0-); **N**) Adenocarcinoma of pancreas (1+); **O**) Metastatic adenocarcinoma from rectum found in liver (2+); **P**) Retinoblastoma (3+). All images were taken at 40x.

positive control for ICAM-1 immunoreactivity, as well as for the isotype negative control tissue. The negative control tissue treated with control rabbit IgG (**Figure 1A**) had no staining in comparison to the positive control tissue treated with anti-ICAM-1 antibody (**Figure 1B**) which had pronounced ICAM-1 staining throughout the tissue. ICAM-1 staining was also seen in a variety of other normal tissue types. Low levels of ICAM-1 staining were observed in normal human testes (**Figure 1C**) as well as normal human thyroid (**Figure 1D**). Both examples of normal human testes and thyroid shown received an ICAM-1 score of 1. Examples of normal human cerebellum (**Figure 1E**), normal human parathyroid (**Figure 1F**), and normal human pituitary (**Figure 1G**) had moderate ICAM-1 staining, all receiving ICAM-1 scores of 2. Normal human colon (**Figure 1H**) was found to be ICAM1 negative, but exhibited ICAM-1 positive immune cells.

A variety of patterns of ICAM-1 staining were observed in malignant and metastatic tumors (**Figure 1**). In some cases, ICAM-1 staining was either surrounding clusters of cells (**Figure 1I**) or on the surface of individual cells (**Figure 1J**). In other cases, ICAM-1 staining was perinuclear (**Figure 1K**), staining either the nucleus or nucleolus. In some tissues, lymphoid cells positively stained for ICAM-1 were seen infiltrating tumors (**Figure 1L**).

Table 1 ICAM-1 expression in normal human tissues

Tissue	ICAM-1 score	Tissue	ICAM-1 score	Tissue	ICAM-1 score	Tissue	ICAM-1 score
Cerebrum	0	Ovary	0	Spleen	3	Esophagus	0
Cerebellum	1.67	Breast	0	Tonsil	2	Small intestine	0
Nerve	0	Uterus	0	Thymus gland	1.67	Colon	0
Adrenal gland	2.33	Uterine cervix	0	Bone marrow	0	Liver	0
Pancreas	0	Testes	1	Heart	0	Salivary gland	0.5
Parathyroid gland	2	Prostate	0	Striated muscle	0		
Pituitary gland	2	Lung	0	Kidney	0.33		
Thyroid	1	Larynx	0	Mesothelium	0		

ICAM-1 scores were based on a scale of 0-3 and positively stained infiltrating lymphocytes were not considered in the overall score for each tissue. Tissues negative for ICAM-1 received an ICAM-1 score of 0 (**Figure 1M**). Tissues that had low levels of ICAM-1 staining received an ICAM-1 score of 1 (**Figure 1N**) and those that had moderate ICAM-1 expression received ICAM-1 scores of 2 (**Figure 1O**). Tissues that received an ICAM-1 score of 3 (**Figure 1P**) had pronounced ICAM-1 staining throughout the tissue.

ICAM-1 staining in normal tissue types and cells is summarized in **Tables 1** and **2**. Of the twenty-nine normal tissue types analyzed, the spleen had the highest level of ICAM-1 expression receiving an average ICAM-1 score of 3. Tissue samples from the adrenal gland, parathyroid gland, pituitary gland, and tonsils, all had average ICAM-1 scores of 2 or above. ICAM-1 expression was absent in the cerebrum, peripheral nerves, pancreas, ovary, breast, uterus, cervix, prostate, lung, larynx, bone marrow, striated muscle, heart, mesothelium, esophagus, small intestine, colon and liver. Epithelial cells in the esophagus, small intestine, colon, cervix, uterus, kidney tubules and lungs were negative for ICAM-1, where as those in the thyroid were positive. We also observed ICAM-1 positive staining in Leydig and germ cells of the testes, adrenal cortex cells, parathyroid chief cells, and cerebellar granular cells.

Table 2 ICAM-1 expression in specific cell types of normal human tissues

Epithelial cells		Other cells		Neuronal cells	
Tissue	ICAM-1	Tissue	ICAM-1	Tissue	ICAM-1
Esophagus	-	Hepatocytes	-	Cerebellar granular cells	+
Cervix	-	Sertoli cells	-	Cerebellar Purkinje cells	-
Uterus	-	Leydig cells	+	Adrenal medulla	-
Lungs	-	Germ cells	+		
Colon	-	Adrenal cortex	+		
Small intestine	-	Muscle (cardiac, skeletal)	-		
Kidney tubules	-	Parathyroid chief cells	+		
thyroid	-				

A

Tumor Type	Ave ICAM-1 Score	Proportion of Samples with Infiltrate
Connective Tissue/Skin	1.07	3/15
Glandular	1.17	1/6
Brain	1.20	0/5
Urinary	1.60	0/5
Digestive	1.78	7/23
Respiratory	2.08	6/13
Female Reproductive	2.08	8/12
Male Reproductive	2.40	1/5
Lymphoid	2.71	7/7
Nephroblastoma	1.50	4/20
Retinoblastoma	1.80	9/20
Neuroblastoma	1.85	4/10
Leukemia	2.2	8/10

B

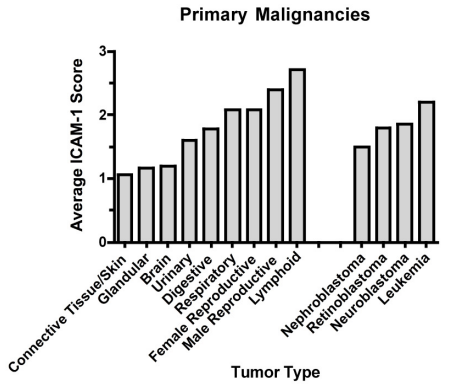

C

Tumor Type	Ave ICAM-1 Score	Proportion of Samples with Infiltrate
Metastases Origin		
Glandular	1.38	4/8
Male Reproduction	1.50	1/2
Respiratory	1.58	5/12
Female Reproduction	1.68	8/19
Digestive	1.85	5/20
Connective Tissue/Skin	2.2	3/5
Urinary	2.25	4/8
Metastases Destination		
Non-Lymphoid Tissue	1.67	18/60
Lymphoid Tissue	2.29	13/14

D

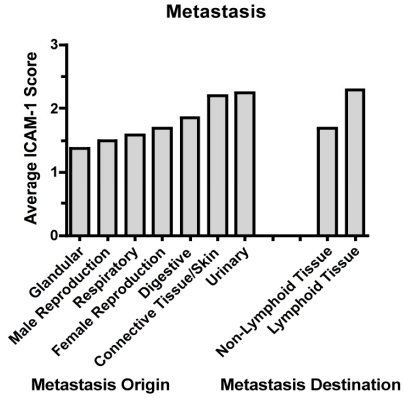

Figure 2 Average ICAM-1 scores and proportion of samples with ICAM-1 positive immune cell infiltrate in various tumor categories for primary (**A**-**B**) and metastatic (**C**-**D**) malignancies.

The expression of ICAM-1 in primary malignant tumors varied greatly amongst different tumor types (**Figure 2**). Lymphoid tumors had the highest levels of ICAM-1 expression (2.71) followed by tumors in the male reproductive tract (2.40). Tumors of connective tissue/skin and glandular malignancies had the lowest level of ICAM-1 expression, with average ICAM-1 scores of 1.07 and 1.17 respectively.

All tumor categories except the brain and urinary tract had tissues with infiltrating lymphocytes and all samples of tumors from the lymphatic system had infiltrate. Other than tumors from the lymphatic system, tumors from the female reproductive tract had the most tissues with infiltrate, with 8 out of 12 tissues possessing infiltrating lymphoid cells.

We further assessed ICAM-1 expression in leukemia and three specific types of blastic tumors: nephroblastoma, neuroblastoma, and retinoblastoma (**Figure 2**). ICAM-1 expression in these malignancies is summarized in **Figure 2**. Of these 4 specific malignancies, leukemia samples had the most ICAM-1 expression with an average ICAM-1 score of 2.20, followed by neuroblastoma, retinoblastoma, and nephroblastoma, which had average ICAM-1 scores of 1.85, 1.80, and 1.50 respectively. All four of these malignancies had samples with infiltrating lymphoid cells, with 8 out of 10 leukemia samples having infiltrate.

ICAM-1 expression in a variety of metastatic malignancies was also assessed and is summarized in **Figure 2**. Metastases originating in urinary tract tissues had the highest level of ICAM-1 expression with an average ICAM-1 score of 2.25 (**Figures 2C** and **D**). Metastases originating from connective tissue/skin had the second highest level of

ICAM-1 expression followed by those originating in the digestive tract, with average ICAM-1 scores of 2.20 and 1.85 respectively. The lowest levels of ICAM-1 expression were found in metastases originating from glandular tissues followed by those originating from the male reproductive tract with average ICAM-1 scores of 1.38 and 1.50 respectively. Malignant metastases localized to lymphoid tissues such as the spleen or lymph nodes had a higher average ICAM-1 score (2.29) in comparison to malignant metastases residing in non-lymphoid tissue (1.67). All originating tumor categories of metastases had tissues with infiltrate, with metastases originating in connective tissue/skin having the highest number of tissues with infiltrate (3 out of 5 tissues). Metastases localized to lymphoid tissue had more samples with infiltrate than those localized to non-lymphoid tissues.

Discussion

The goal of this study was to carry out a comprehensive survey investigating the expression of ICAM-1 in various normal, malignant and metastatic tissues. Due to its presence on many cancer cell types [1, 5, 6, 7, 8], upregulation of its soluble form in cancer patients [3, 4] and potential role in metastasis [7, 9, 10, 11], ICAM-1 expression may serve as an important diagnostic tool for assessing tumor prognosis and progression as well as its potential as a target for therapeutic intervention.

In our analysis of ICAM-1 expression in normal tissues, we found that ICAM-1 immunoreactivity is not ubiquitous, but is limited to specific tissue and cell types. ICAM-1 expression was absent in a variety of normal tissue types including the cerebrum, peripheral nerves, pancreas, ovary, breast, uterus, cervix, prostate, lung, larynx, bone marrow, striated muscle, heart, mesothelium, esophagus, small intestine, colon and liver. The normal tissue type exhibiting the highest level of ICAM-1 immunoreactivity was the spleen, as normal lymphoid cells are known to constitutively express ICAM-1 at low levels [4]. Smith and Thomas [12] have previously reported the expression of ICAM-1 in some normal cell and tissue types and our results are in congruence with some of their earlier findings. Some of our findings, however, differ from the findings of Smith and Thomas. For example, we observed ICAM-1 expression in Leydig cells and germ cells of the testes, epithelium of the thyroid, and granular cells of the cerebellum, all of which were reported ICAM-1 immunonegative in the earlier study. Smith and Thomas also report ICAM-1 staining in liver hepatocytes and kidney tubules, both of which we observed to be ICAM-1 negative. One potential cause for the discrepancy between our findings was the specific ICAM-1 antibody that was used. It is possible that the rabbit polyclonal antibody used in our study detected more ICAM-1 epitopes than the mouse monoclonal antibody used by Smith and Thomas. Furthermore, in the Smith and Thomas study, in some cases, only one tissue sample was analyzed for ICAM-1 expression, whereas we analyzed multiple samples per tissue type and calculated an overall average ICAM-1 score for each tissue. It is possible that the single tissue samples analyzed by Smith and Thomas may not have been representative for all tissues of that type.

During the investigation of malignant and metastatic tumors, we observed a number of different patterns of ICAM-1 staining. In some tissues ICAM-1 staining was found around clusters of cells, which may represent adsorbed soluble protein, and in others it was found on the surface of individual cells. We also observed ICAM-1 staining in a number of tissues that was perinuclear although the significance of this staining pattern is not known. We have also observed this pattern of staining in paraffin embedded retinoblastoma samples that are not part of commercial tissue micro-arrays (Supplementary Figure 1). Additionally, many malignant and metastatic samples displayed ICAM-1 positive lymphoid cells infiltrating the tumor tissues, indicative of an immune response. Of the primary malignancies analyzed, tumors from the female reproductive tract as well as leukemia samples had the highest number of samples with infiltrate. Of the primary malignancies analyzed, none of the samples from the brain or the urinary tract had infiltrating lymphocytes. The observation that there were no infiltrating lymphoid cells in the brain can be explained by the actions of the blood-brain barrier, which is responsible for restricting the movement of immune cells from the circulating blood stream to the tissues of the brain [13]. Similarly, the blood-retinal barrier is responsible for restricting the movement of molecules and immune cells between the circulating blood and the retina [14, 15].

Infiltrating immune cells were observed in a number of retinoblastoma samples indicating that retinoblastoma tumors may interfere with or disrupt the blood-retinal barrier. Of the metastatic tumors, tissues originating from the connective tissue/skin category had the highest number of samples with infiltrate. Metastatic tumors localized in lymphoid tissues had high levels of infiltrate in comparison to those localized to non-lymphoid tissues. This is most likely due to the proximity of immune cells within lymphoid tissues available to infiltrate tumors.

Through our investigation of malignant and metastatic tumors we also observed varying levels of expression of ICAM-1 in different tissue and tumor types. Of the primary malignancies analyzed, tumors of the lymphatic system had the highest average ICAM-1 scores. The higher levels of ICAM-1 seen in lymphoid tumors is most likely due to the fact that ICAM-1 is normally found in lymphoid tissues [4] and would seem to be a conducive environment for ICAM-1 expression. Of the metastatic tumors analyzed, tumors originating in the urinary tract had the highest average ICAM-1 score and tumors localized to lymphoid tissues showed more ICAM-1 immunoreactivity than those localized to non-lymphoid tissues. Furthermore, of all the primary malignancies in our study, those from connective tissue/skin received the lowest average ICAM-1 score and of the metastatic tumors we investigated, those originating in glandular tissues received the lowest average ICAM-1 score. The observed differences in the expression of ICAM-1 amongst different tissue types as well as between primary and metastatic malignancies is not well understood, but would be an interesting area for further investigation.

Adhesion molecules such as ICAM-1 have been implicated in playing a role in cancer metastasis [7, 9, 10, 11]. The regulation of ICAM-1 expression by cancer cells may facilitate the process of metastases, whereby invasive cells dissociate from a tumor proper, enter circulation, avoid being targeted by immune cells, and attach and invade distal sites [3]. The regulation of ICAM-1 in metastatic cancer cells has also been associated with the ability of metastatic cells to be resistant to lysis by immune cells [16]. By down-regulating ICAM-1 expression, metastatic cells were able to escape specific immune cell-mediated killing. Lin *et al* [7] have previously investigated the expression of ICAM-1 in various human lung cancer samples and have reported a correlation between the level of ICAM-1 expression in tumor samples with advanced stages of lung cancer and metastasis. Lung cancer patients who had tumors with high levels of ICAM-1 expression were likely to have a more advanced stage of lung cancer and metastases to other parts of the body.

Due to its association with the process of metastasis, ICAM-1 has been a target for therapeutic intervention in several studies. A novel anti-ICAM-1 blocking antibody, UV3, has been used experimentally on human xenografts to study ICAM-1 blocking effects on tumor progression and survival in SCID mice [9, 11]. Administration of UV3 to mice with human xenografts slowed the growth of breast, non-small cell lung, pancreatic, and prostate tumors and increased survival time of mice with multiple myeloma, lymphoma, and melanoma xenographs. Lin *et al* [7] have also reported that Thalidomide, which was found to inhibit TNF-α induced expression of ICAM-1, was effective in decreasing in vivo metastasis of human lung cancer in mice.

In summary, we have presented a comprehensive study on the immunoreactivity of ICAM-1 in normal, malignant and metastatic tissues. Since ICAM-1, both in its soluble and cell-associated forms, seems to play a role in tumor progression and metastasis, our findings should serve as a helpful resource for investigations of ICAM-1 as a biomarker and a potential target for therapeutic interventions.

Acknowledgements

This work was supported by R21CA127061, a departmental challenge grant and a Sybil Harrington Research Scholar grant from Research to Prevent Blindness, as well as a Vision Research core infrastructure grant 1R24EY016662. We would also like to thank Dr. Cynthia Dlugos for her assistance with histological analysis.

Please address all correspondences to Gail M. Seigel, Ph.D., Department of Ophthalmology, Ross Eye Institute, University at Buffalo, 3435 Main Street, Sherman 124, Buffalo, NY 14214. Tel: 716-829-5216; Fax: 716-829-2344; Email: gseigel@frontiernet.net

References

[1] Dymicka-Piekarska V and Kemona H. Does colorectal cancer clinical advancement affect adhesion molecules (sP- selectin, sE- selectin and ICAM-1) concentration? *Thromb Res* 2009 [Epub ahead of print]

[2] Yang L, Froio RM, Sciuto TE, Dvorak AM, Alon R and Luscinskas FW. ICAM-1 regulates neutrophil adhesion and transcellular migration of TNF-alpha-activated vascular endothelium under flow. *Blood* 2005;106: 584-592.

[3] Basoglu M, Atamanalp SS, Yildirgan MI, Aydinli B, Ozturk G, Akcay F and Oren D. Correlation between the serum values of soluble intercellular adhesion molecule-1 and total sialic acid levels in patients with breast cancer. *Eur Surg Res* 2007;39:136-140.

[4] Dowlati A, Gray R, Sandler AB, Schiller JH and Johnson DH. Cell adhesion molecules, vascular endothelial growth factor, and basic fibroblast growth factor in patients with non-small cell lung cancer treated with chemotherapy with or without bevacizumab–an Eastern Cooperative Oncology Group Study. *Clin Cancer Res* 2008; 14:1407-1412.

[5] Choi Y-L, Xuan YH, Shin YK, Chae SW, Kook MC, Sung RH, Youn SJ, Choi JW and Kim SH. An immunohistochemical study of the expression of adhesion molecules in gallbladder lesions. *J Histochem Cytochem* 2004;52:591-601.

[6] Hemmerlein B, Scherbening J, Kugler A, and Radzun H-J. Expression of VCAM-1, ICAM-1, E- and P-selectin and tumour-associated macrophages in renal cell carcinoma. *Histopathology* 2000;37:78-83.

[7] Lin Y-C, Shun C-T, Wu M-S and Chen C-C. A novel anticancer effect of Thalidomide: Inhibition of intercellular adhesion molecule-1 mediated cell invasion and metastasis through suppression of nuclear factor-kB. *Clin Cancer Res* 2006;12:7165-7173.

[8] Tempia-Caliera AA, Horvath LZ, Zimmermann A, Tihanyi TT, Korc M, Friess H and Buchler MW. Adhesion molecules in human pancreatic cancer. *J Surg Oncol* 2002;79:93-100.

[9] Brooks KJ, Coleman EJ and Vitetta ES. The antitumor activity of an anti-CD54 antibody in SCID mice xenographed with human breast, prostate, non-small cell lung, and pancreatic tumor cell lines. *Int J Cancer* 2008;123: 2438-2445.

[10] Liang S, Slattery MJ, Wagner D, Simon SI and Dong C. Hydrodynamic shear rate regulates melanoma-leukocyte aggregation, melanoma adhesion to the endothelium, and subsequent extravasation. *Ann Biomed Eng* 2008;36: 661-671.

[11] Wang S, Coleman EJ, Pop LM, Brooks KJ, Vitetta ES and Niederkorn JY. Effect of an anti-CD54 (ICAM-1) monoclonal antibody (UV3) on the growth of human uveal melanoma cells transplanted heterotopically and orthotopically in SCID mice. *Int J Cancer* 2006;118:932-941.

[12] Smith MEF and Thomas JA. Cellular expression of lymphocyte function associated antigens and the intercellular adhesion molecule-1 in normal tissue. *J Clin Pathol* 1990;43:893-900.

[13] Stolp HB and Dziegielewska KM. Review: Role of developmental inflammation and blood-brain barrier dysfunction in neurodevelopmental and neurodegenerative diseases. *Neuropathol Appl Neurobiol* 2009;35: 132-146.

[14] Madigan MC and Penfold PL. Human retinoblastoma: a morphological study of apoptotic, leukocytic, and vascular elements. *Ultrastruct Pathol* 1997;21:95-107.

[15] Greenwood J, Pryce G, Devine L, Male, DK, dos Santos WLC, Calder VL and Adamson P. SV40 large T immortalized cell lines of the rat blood-brain and blood-retinal barriers retain their phenotypic and immunological characteristics. *J Neuroimmun* 1996;71: 51-63.

[16] Hamai A, Meslin F, Benlalam H, Jalil A, Mehrpour M, Faure F, Lecluse Y, Vielh P, Avril M, Robert C and Chouaib S. ICAM-1 has a critical role in the regulation of metastatic melanoma tumor susceptibility to CTL lysis by interfering with PI3K/AKT pathway. *Cancer Res* 2008;68:9854-9864.